

ATLAS Tile Calorimeter: simulation and validation of the response

Jana Faltova, on behalf of the ATLAS Collaboration

Charles University in Prague, Institute of Particle and Nuclear Physics, Czech Republic

E-mail: jana.faltova@cern.ch

Abstract. The Tile Calorimeter (TileCal) is the central section of the ATLAS hadronic calorimeter at the Large Hadron Collider. Scintillation light produced in the tiles is readout by wavelength shifting fibers and transmitted to photomultiplier tubes (PMTs). The resulting electronic signals from approximately 10000 PMTs are measured and digitized before being further transferred to off-detector data-acquisition systems. Detailed simulations are described in this contribution, ranging from the implementation of the geometrical elements to the realistic description of the electronics readout pulses, including specific noise treatment and the signal reconstruction. Special attention is given to the improved optical signal propagation and the validation with the real particle data.

1. Introduction

The Tile Calorimeter [1] is a central hadronic calorimeter in the ATLAS detector [2] at the LHC. It consists of a barrel (in the pseudorapidity region $|\eta| < 1.0$) and two extended barrels ($0.8 < |\eta| < 1.7$). It covers the area from 2280 to 3865 mm in the radial direction. The TileCal is a sampling calorimeter with alternating scintillating tiles (active medium) and steel (absorber). The calorimeter is segmented into three-dimensional cells. There are three radial layers (denoted as A, BC, D) and fine segmentation in $\Delta\eta \times \Delta\phi$ (0.1×0.1 in A, BC cells and 0.2×0.1 in D cells). Light emitted in the scintillator is transmitted by the wavelength shifting fibers to the photomultipliers. Each calorimeter cell is read out by two photomultipliers on both ϕ -sides of the cell.

Simulations of the Tile Calorimeter can be divided into three parts — simulation, digitization and reconstruction. The Geant4 toolkit [3, 4] is used in the simulation step. The geometry of the detector is thoroughly described and the passage of particles through matter is simulated. Collection of hits (energy deposits characterized by its position, energy and time) is created and used as the input for the digitization. Next, hits from the signal sample and hits from the minimum bias background events (in-time and out-of-time pile-up) are merged together in one collection. Seven samples spaced by 25 ns are derived corresponding to the situation in real data. Electronic noise is added to the individual samples. Thereafter, the read-out samples are processed in the reconstruction which is identical to the procedure applied in data. The energy is reconstructed by means of the Optimal Filtering Method and the cell energy is calibrated to the electromagnetic scale.



2. Noise description

Two main sources of disturbance might degrade the physics signal — electronic noise and a contribution from multiple minimum bias collisions overlaid with the hard scattering process (the pile-up). Good description of the noise is important for the creation of so-called topoclusters (clusters of cells based on noise significance) that are used for building the physics objects, especially hadronic jets.

The electronic noise was measured in data and found to have significant non-Gaussian tails. The cell noise is approximated with a double Gaussian function to a good precision. The double Gaussian model is used also in the Monte Carlo simulations where the noise is added to the individual samples. The constants used in the simulations are derived from the measurements in data cell by cell. A good agreement between data and Monte Carlo simulations is achieved as can be seen in figure 1. The measurement was performed using 2010 data where the pile-up term can be neglected. The noise contribution can be compared with data collected using a random trigger. The electronic noise comes mainly from the Low Voltage Power Supply (LVPS) which provides power to the front-end electronics. A new version of the LVPS is being installed and will be used for the next data-taking period (Run 2). The new LVPS lead to smaller electronic noise with more Gaussian behavior.

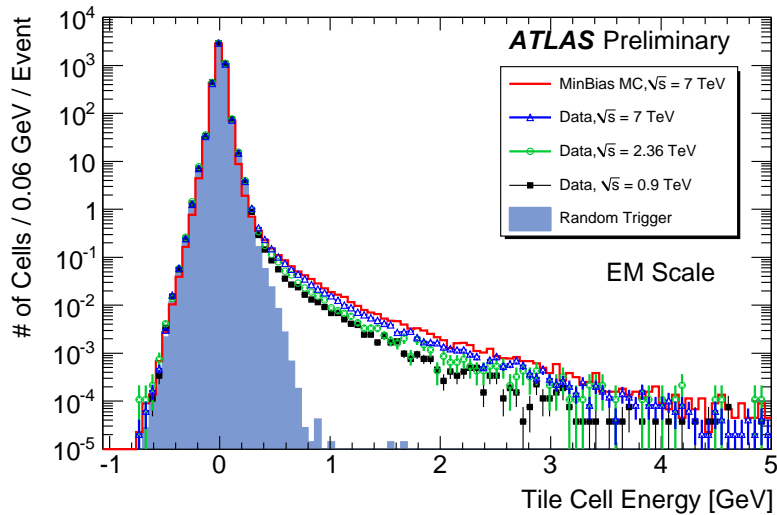


Figure 1. Cell energy spectrum measured in 2010 data. The pile-up term might be neglected.

Contrary to the electronic noise, the pile-up noise depends strongly on the radial layer. The largest contribution affects the A-cells (closest to the beam pipe) while the smallest pile-up appears in D-layer cells. Moreover, strong dependence on the pseudorapidity was found as shown in figure 2, where the noise level for all three radial layers (A, BC, D) and the gap/crack scintillators is plotted. The observed agreement between data and simulations is within $\pm 20\%$ in the region where pile-up is dominant. Currently, a simple model evaluates the pile-up term using the standard deviation of the cell energy distribution, the shape is not considered. An improved model, which takes into account the pile-up energy spectrum shape, is being prepared to be used in Run 2.

3. Optical signal propagation

The response of the photomultipliers is not flat in the azimuthal angle difference between the energy deposition point and the center of the cell ($\Delta\phi$), but it shows a non-negligible dependence

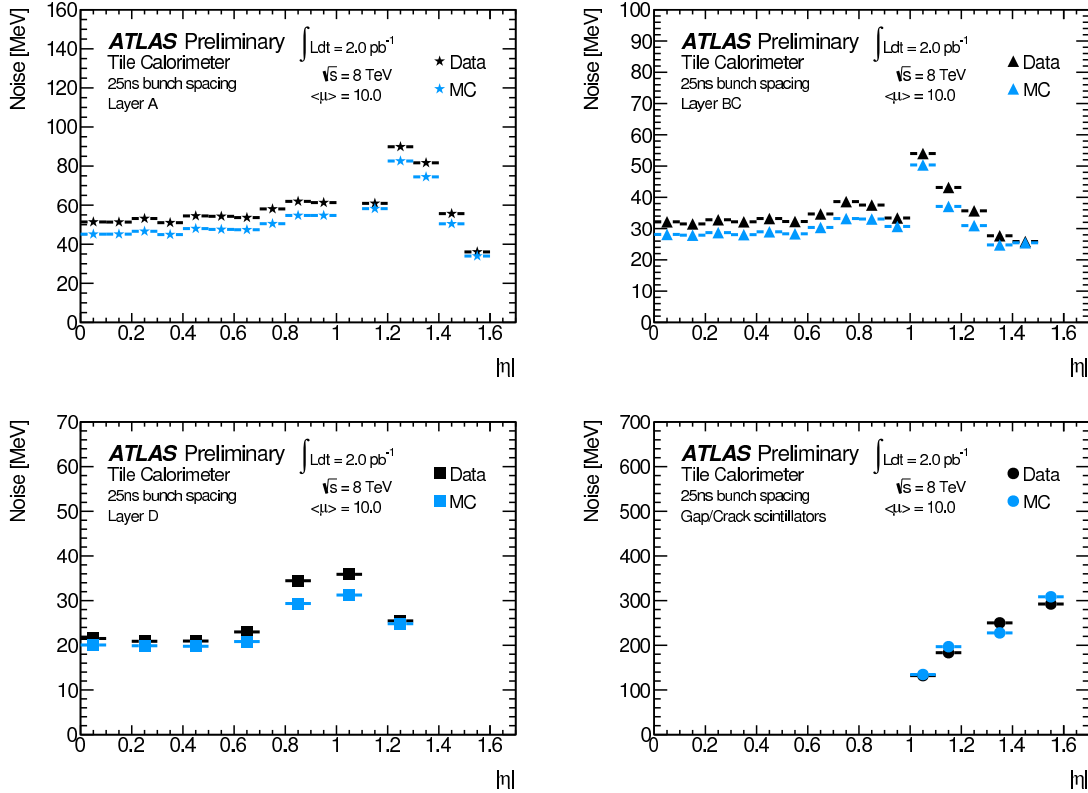


Figure 2. Cell noise distribution in the presence of pile-up measured with data collected at a centre-of-mass energy of 8 TeV with a bunch spacing of 50 ns and an average number of interactions 15.7 per bunch crossing.

60 referred to as U-shape. The dependence of the response on $\Delta\phi$ was measured using $W \rightarrow \mu\nu$
61 events in the 2012 collisions data. The measurement is performed separately in the barrel and
62 in the extended barrels in each radial layer. The typical shape is shown in figure 3 (a) for barrel
63 and 3 (b) for extended barrel. A steep dip at the center of the cell ($\Delta\phi = 0$) corresponds to
64 the position of the apertures in the scintillating tiles¹. The decrease at the edges of the cells
65 ($\Delta\phi > 0.03$) is due to the geometrical effects.

66 The U-shape option has been recently added in the Monte Carlo simulations. Look-up tables
67 were prepared based on the measurements in data and used in the simulations. The tables are
68 normalized as follows: First, average value for one PMT is set to 0.5. Second, the look-up tables
69 are rescaled to have the same sampling fraction for 100 GeV electrons at $\eta = 0.35$ in the center
70 of the cell as the simulations without the U-shape. The comparison between simulations with
71 and without U-shape can be seen in figures 4 (a) to (f). The layers A, BC and D in the central,
72 resp. extended barrel are shown in figures (a), (b) and (c), resp. (d), (e) and (f).

73 4. Comparison between data and Monte Carlo simulations

74 4.1. Validation of the electromagnetic scale

75 The electromagnetic scale (EM) in TileCal is calibrated using electron beam data at the angle of
76 20 degrees. The validation of the EM scale was done using muons and pions in test beams and

¹ Each scintillating tile has two apertures in its phi-center. While a large rod runs through one hole and physically fixes the tile in the iron structure, a pipe used by Cesium calibration system is running through the second hole.

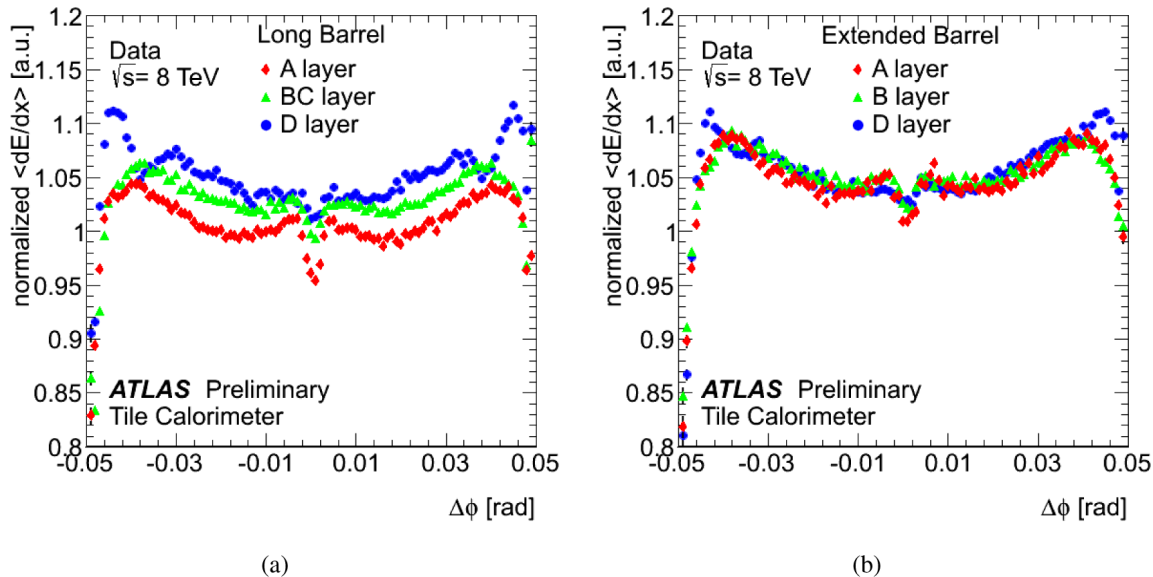


Figure 3. Response dependence on the azimuthal angle difference between the muon track impact point and the center of the cell ($\Delta\phi$) measured in 2012 collisions data using $W \rightarrow \mu\nu$ events.

77 also cosmic muons, details can be found in [1, 5]. As an example, an analysis with cosmic muons
 78 is discussed here. A very good separation between signal and noise is achieved with S/N ratio
 79 of 29 for the sum of the three radial layers as shown in figure 5. The cell response uniformity,
 80 in terms of dE/dx , was measured with the muon tracks and was found to be better than 5%
 81 in all three layers. The EM scale measurement was compared with test beam results and it is
 82 consistent with each other within an uncertainty of 4%. The ratio of data and Monte Carlo
 83 predictions is close to one, as required (see figure 6).

84 4.2. Measurements of E/p ratio

85 The calorimeter response can be characterised by the ratio of energy and momentum (E/p)
 86 for isolated tracks. The deposited energy E is measured in the calorimeter while momentum p
 87 in the inner tracker. The energy reconstructed in the electromagnetic calorimeter is required
 88 to be smaller than 1 GeV in order to find hadrons with most of their energy in TileCal. The
 89 results using 2011 collision data are shown in figure 7. A good agreement between data and
 90 Monte Carlo predictions is observed. The largest difference of 10% occurs in the gap region
 91 ($0.9 < |\eta| < 1.1$) where a precise description of the detector material is very difficult.

92 5. Conclusions

93 Data collected in TileCal have been compared with Monte Carlo simulations in a wide range
 94 of measurements — test beams, cosmic, collisions data. A good level of agreement was found
 95 at low signals (corresponding to noise contribution) and also at high energy signals. The light
 96 propagation in the Monte Carlo simulations has been improved by introducing the U-shape.
 97 Furthermore, more precise pile-up description will be used in the next data taking period.

98 References

- 99 [1] Atlas Collaboration 2010, *Eur.Phys. J. C* **70** 1193
 100 [2] Atlas Collaboration 2008, *JINST* **3** S08003
 101 [3] Agostinelli, S. et al. 2003, *Nuclear Instruments and Methods in Physics Research A* **506** 250-303

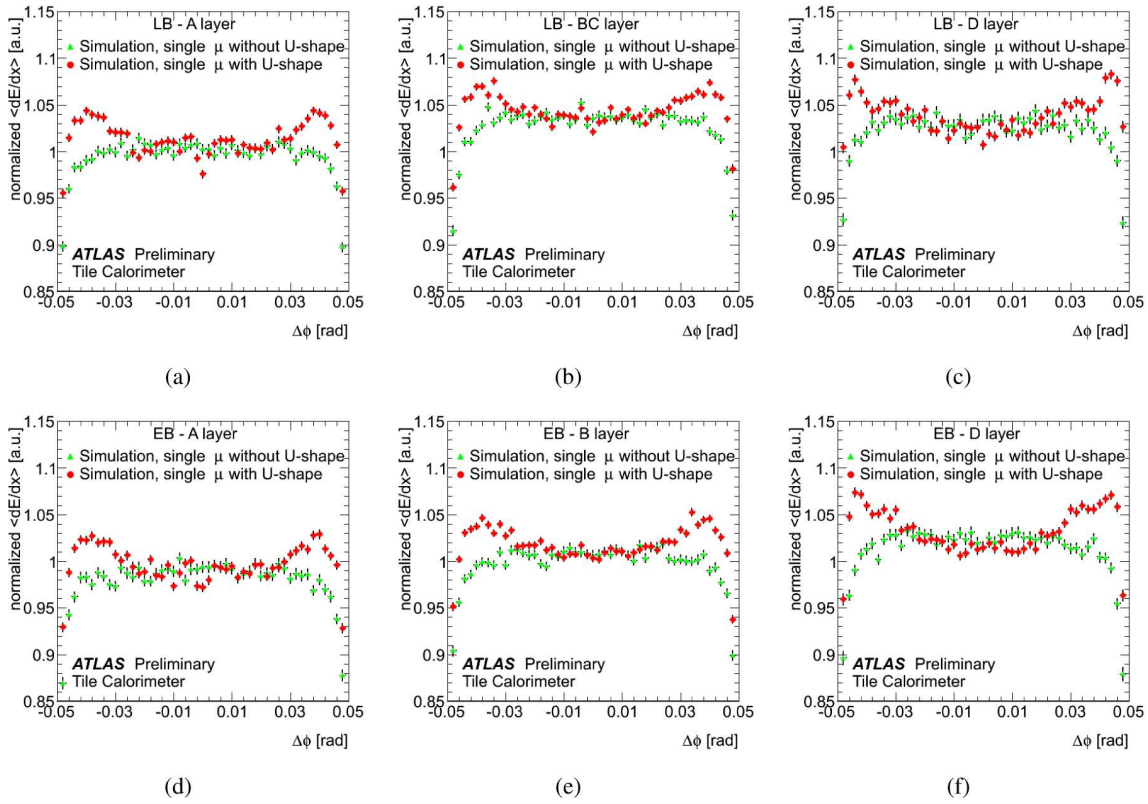


Figure 4. Response dependence on the azimuthal angle difference between the muon track impact point and the center of the cell ($\Delta\phi$) for Monte Carlo simulations with (red color) and without (green color) the U-shape.

102 [4] Allison, J. et al. 2006, *IEEE Transactions on Nuclear Science* 53 No. 1 270-278

103 [5] Atlas Collaboration 2009, *Nuclear Instruments and Methods in Physics Research A* 606 362-394

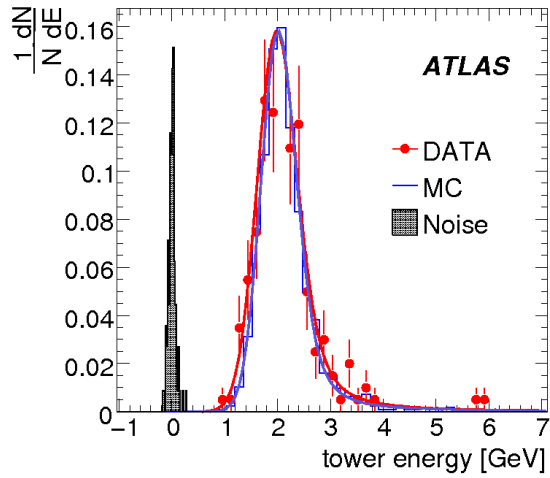


Figure 5. Example of the muon signal and noise for projective cosmic muons at $0.3 < |\eta| < 0.4$.

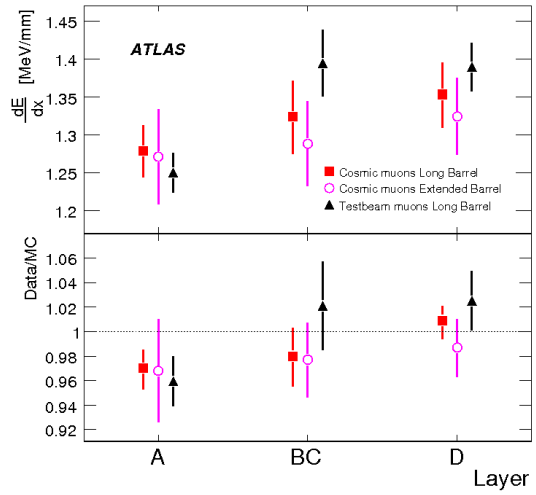


Figure 6. The truncated mean of the dE/dx for cosmic and test beam muons per radial layer. Comparison with Monte Carlo simulations is shown in the bottom part of the plot.

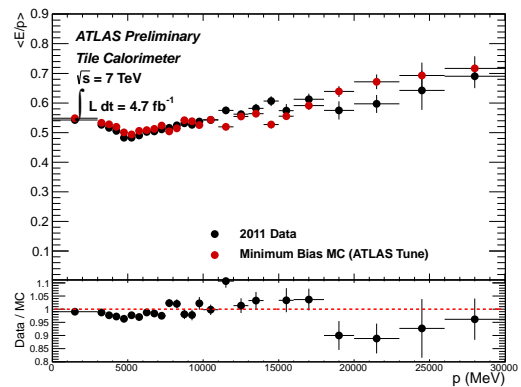
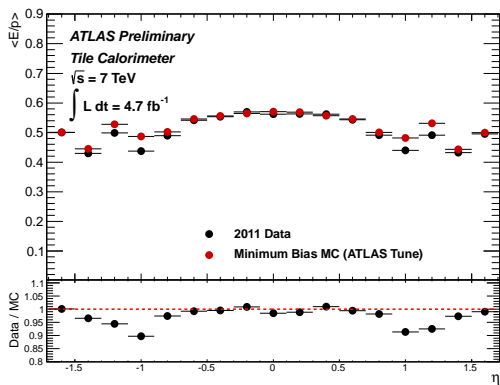


Figure 7. Energy over momentum (E/p) for isolated tracks using proton-proton collision data from 2011. The dependence on the pseudorapidity (momentum) is shown in the left (right) plot.